

Article

Not peer-reviewed version

Cutting Power Model Determination for Solid Wood Processing Using Response Surface Methodology

[Miran Merhar](#)*, [Damir Hodžić](#), [Redžo Hasanagić](#), Nedim Hurem, Atif Hodžić

Posted Date: 19 December 2025

doi: 10.20944/preprints202512.1710.v1

Keywords: cutting force; energy consumption; milling; tool; woodworking



Preprints.org is a free multidisciplinary platform providing preprint service that is dedicated to making early versions of research outputs permanently available and citable. Preprints posted at Preprints.org appear in Web of Science, Crossref, Google Scholar, Scilit, Europe PMC.

Copyright: This open access article is published under a [Creative Commons CC BY 4.0 license](#), which permit the free download, distribution, and reuse, provided that the author and preprint are cited in any reuse.

Disclaimer/Publisher's Note: The statements, opinions, and data contained in all publications are solely those of the individual author(s) and contributor(s) and not of MDPI and/or the editor(s). MDPI and/or the editor(s) disclaim responsibility for any injury to people or property resulting from any ideas, methods, instructions, or products referred to in the content.

Article

Cutting Power Model Determination for Solid Wood Processing Using Response Surface Methodology

Miran Merhar ^{1,*}, Damir Hodžić ², Redžo Hasanagić ², Nedim Hurem ² and Atif Hodžić ²

¹ University of Ljubljana, Biotechnical Faculty, Department of Wood Science and Technology, Slovenia;

² University of Bihać, Faculty of Technical Engineering, Bosnia and Herzegovina

* Correspondence: miran.merhar@bf.uni-lj.si

Abstract

In the study, a model was developed to calculate the power required for the circumferential cutting of solid wood in the longitudinal direction, considering the relevant technological parameters and mechanical properties of the wood. Based on measurements of different combinations and using the Response surface method (RSM) and the Central composite design (CCD), a model was created that, in its derived version, considers the cutting width and depth, the diameter and speed of the tool, the number of cutting edges and the sharpness of the cutting edge, the feed rate of the workpiece and the density and moisture content of the wood. The model can be used to calculate the cutting power of various tree species with densities ranging from 400 to 700 kg/m³, moisture contents from 8 to 16%, and a wide range of cutting-edge sharpness, from a sharp cutting edge with a tip radius of 5 µm to a blunt cutting edge with a tip radius of 35 µm. The model is designed for a rake angle of 20°, the value most frequently used in practise. An ANOVA analysis was used to determine the suitability of the model, which is highly significant with an R² value of 0.93 and an average deviation of the calculated values from the measured values of 8.8%. The model is robust and therefore useful in the wood industry for predicting energy consumption in the processing of solid wood.

Keywords: cutting force; energy consumption; milling; tool; woodworking

1. Introduction

1.1. Literature Overview

Energy consumption is an important factor and the general aim is to minimise energy consumption. In certain cases, the goal is to optimise energy consumption so that the capacity of a given process is as high as possible for a given energy consumption, or in another case, to reduce energy consumption for a given capacity. However, minimising energy consumption is not always the most important factor, e.g. if a certain product has to be manufactured to the required quality, even if the energy consumption is higher than it would otherwise be.

Regardless of the situation, it is necessary to know which factors influence energy consumption. With an appropriate model, these factors can be optimised so that energy consumption is optimal in certain cases, or energy consumption can be planned if certain factors are set in order to achieve the desired processing quality.

When processing wood, various factors influence the cutting force and therefore the energy consumption. Among the technological factors, the cutting force is influenced by the cutting depth and width, the tool diameter, the number of cutting edges, the rotational speed of the tool and the feed rate [1-6]. These factors interact in various ways and influence the thickness of the chip and the cutting direction in relation to the grain of the wood, which in turn has a direct effect on the cutting force. In addition, the cutting force is also influenced by the rake angle of the blade [7,8], the sharpness of the blade [9], and the friction between the blade and the wood [10,11], over which the production engineer has little or no direct influence. The cutting force decreases as the rake angle increases, but

the rake angles in solid wood processing are generally not greater than 20-25° and are on average between 18 and 22°. Longitudinal cutting of solid wood with a rake angle of more than 30° produces a type I chip [12,13], which is characterised by the fact that the tissue is split before the blade tip, i.e. the wood can also be split below the blade tip, resulting in a chipped grain surface, which is undesirable and represents poor machining quality [14]. However, if the rake angle is less than 25° on average, a type II chip is created, which is characterised by the fact that the tissue is not split in front of the tip of the blade, but is created by a combination of pressure and shear failures. In this case, the wood surface is free of chipped grain and represents a better surface quality. The rake angle range of 25 to 30° represents a transitional area in which a type I or II chip can occur. With a smaller rake angle of less than 15°, however, the quality of the machined surface can also be worse, as a type III chip can occur, characterised by a combination of pressure failure and tissue splitting in front of the blade tip.

In addition to the technological factors mentioned above, the cutting force and thus the energy consumption are also influenced by the moisture content [15] and mechanical properties of the wood in various directions, such as elasticity, strength and fracture toughness [16]. Various authors have attempted to model the cutting force considering the various technological and mechanical properties.

The cutting forces were modelled using the finite element method, taking into account the elasticity, strength and fracture properties of the material [17,18], as well as cutting models based on the strains in the material in front of the tool tip [19]. Various attempts were also made to create a cutting model that takes into account fracture properties [20-22] or is based on different failure criteria and chip breakage due to compressive failure [23,24]. Various models were also created for other orthotropic materials like bone [25,26].

Despite extensive research, there is still no universal model that can be used to calculate cutting forces and power for different combinations of technological parameters and mechanical properties of wood. On the other hand, the existing models are quite challenging for industrial technologists, as they need to be familiar with the various mechanical properties of wood, which in certain cases are unknown or hardly available in the generally accessible literature.

An alternative to such models is a mechanistic approach, where the cutting forces are measured based on certain combinations of wood mechanical properties and technological parameters, which can then be used to create a mathematical model that is valid in the tested range on which the model is based. Typically, such models incorporate wood density and moisture content rather than mechanical properties, as there are positive correlations between wood density and its mechanical properties [27].

This approach has been used in numerous studies in which various authors have investigated the effects of different factors on the magnitude of cutting forces or power. Jiang, *et al.* [28] investigated the effects of rake angle, wedge angle and clearance angle at different cutting speeds. The influence of chip thickness and tool wear on cutting power was investigated by Pinkowski, *et al.* [29]. Homkhiew, *et al.* [30] investigated the influence of cutting speed, workpiece feed and cutting depth, while Dvoracek, *et al.* [31] analysed the effects of cutting direction and wood moisture content in linear cutting of oak. Similarly, the influence of blade inclination angle, feed rate and depth of cut was investigated by Jin and Wei [32] and Li, *et al.* [33]. A more thorough study of the influence of various technological parameters and wood properties in linear cutting of wood was carried out by Porankiewicz, *et al.* [34], who created a complex model with more than 50 coefficients. To use the model for circular cutting, the reader must calculate the average thickness of the chip and determine the average cutting angle between the cutting direction and the tissue orientation. The authors have also used the cutting model for other research. For example, Derbas, *et al.* [35] has used the frequency spectrum in cutting to determine the moisture content of wood or its fracture properties [36].

As already mentioned, an alternative is to use different mathematical models, but to the author's knowledge, none of the studies mentioned in the introduction that have been carried out so far have fully captured the effects of all relevant technological factors and wood properties and are at the same time simple, robust and precise. Individual studies have been carried out in which individual authors have created cutting models based on a linear cut under certain conditions. However, these have little

practical value in real technological processes, as the user would have to modify the model and calculate the equivalent thicknesses of the chip resulting from the circular cut. On the other hand, various models based on a circular cutting contain many numerical constants, which can also lead to a high probability of incorrect calculation of the cutting power, or the models do not contain all relevant technological and material properties.

The aim of this research is therefore to create a simple, robust, precise and comprehensive model for calculating the power required for circular circumferential cutting of solid wood in the longitudinal direction, which considers all relevant technological and material properties of wood and is useful for user in the industry. The model will be based on the mechanical properties of wood density and moisture content, and will include all relevant technological parameters, such as cutting depth and width, workpiece feed, tool speed, tool diameter, and the number and sharpness of cutting knives. Compared to the other models mentioned in the cited articles, this model will be simpler and will include all relevant parameters. The aim of the research is to use the Design of Experiment (DOE) approach [37,38] in the development of the model, which makes it possible to design a robust model with many variables and a relatively small number of experimental combinations, while still considering the main influences of the parameters and their mutual interactions.

1.2. Theoretical Background

The basis for the mean cutting force for a single cut can be derived from the relationship between the width b , mean thickness of the chip h_m and a specific coefficient k_s [2]

$$F_m = k_s \cdot b \cdot h_m \quad (1)$$

where the specific cutting coefficient k_s depends on the technological parameters and properties of the wood.

In circular peripheral cutting, the thickness of the chip increases with the angle φ , as shown in Figure 1, which increases the cutting force. When calculating the average cutting force F_m for a single chip, the average chip thickness h_m should be taken into account, which is calculated using the following equation [1]

$$h_m = f_z \cdot \sqrt{\frac{a}{d}} \quad (2)$$

Here, a is the depth of cut (Figure 1), d is the diameter of the tool and f_z is the feed per tooth, which is calculated as follows

$$f_z = \frac{v_f}{n \cdot z} \quad (3)$$

where v_f is the feed speed and n and z are the rotational speed of the tool and the number of cutting knives, respectively.

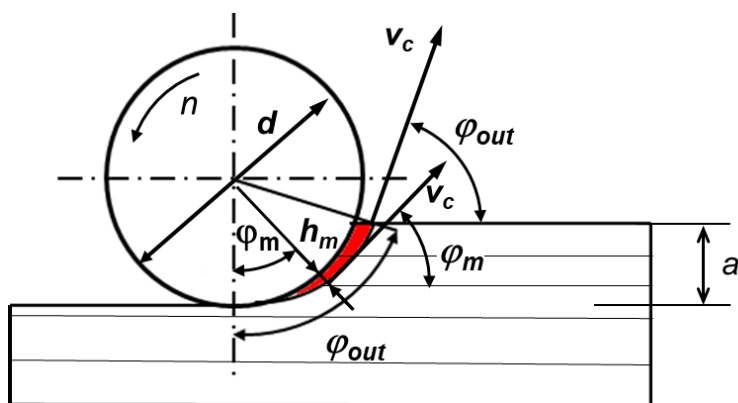


Figure 1. Schematic of cutting principle; v_c – cutting direction vector, a – depth of cut, d – cutting tool diameter, n – tool rotational speed, φ_{out} – tool exit angle, φ_m – mean cutting angle, h_m – mean chip thickness.

In addition to the increase in force due to the increasing chip thickness during circular cutting, the cutting force also increases due to the change in the angle φ between the cutting speed vector v_c and the grain of the wood. For example, the cutting forces are lowest for a longitudinal cut when the angle φ is zero and the velocity vector v_c is parallel to the grain, and highest for a pure cross-section when the angle φ is 90° and the velocity vector is perpendicular to the grain [39].

When calculating the mean cutting force F_m for a single chip during circular cutting, in addition to the changing thickness of the chip, the changing conditions with regard to the cutting direction must also be considered with the corresponding value of the specific cutting force k_s in equation 1, whereby it is most practical to take into account the values k_s at the mean angle φ_m ,

$$\varphi_m = \frac{\varphi_{out}}{2} \quad (4)$$

Here, φ_{out} is the angle between the blade's velocity vector and the grain direction at the point where the knife leaves the workpiece (Figure 1), calculated using the equation

$$\varphi_{out} = \arccos\left(\frac{r-a}{r}\right) \quad (5)$$

where a is the cutting depth and r is the tool radius. If the function is developed into a Taylor series, φ_{out} can be written in simplified form

$$\varphi_{out} = 2 \cdot \sqrt{\frac{a}{d}} \quad (6)$$

When circular cutting a thick workpiece with a tool with a large number of cutting knives, there may be a large number of knives in the workpiece at the same time, such as when sawing with a circular saw, where the circular saw blade may have up to 100 or more cutting knives, or there may be only one or even no knife in the workpiece, such as when peripheral milling or planing workpieces. In this case, the instantaneous cutting force varies from zero, when the knife is not in contact with the wood and is not cutting it, to the maximum force when the knife is cutting and the thickness of the chip is at its greatest. However, the cutting force can also be represented by the average cutting force per chip F_m . If the average cutting power is to be determined, the average cutting force per revolution of the tool must first be determined, which can also be referred to as the operating force F_{op} and is calculated using the following equation

$$F_{op} = F_m \cdot z_{ef} \quad (7)$$

F_m is the mean force per chip and z_{ef} is the average number of cutting knives. For example, z_{ef} can be between 0 and 1 when circumferential milling or planing with tools with a smaller number of cutting knives, where no knife or only one knife cuts at a time, and is calculated using the following equation

$$z_{ef} = \frac{z \cdot \varphi_{out}}{2\pi} = \frac{z \cdot 2 \cdot \sqrt{\frac{a}{d}}}{2\pi} = \frac{z}{\pi} \sqrt{\frac{a}{d}} \quad (8)$$

With the F_{op} the torque M_c and cutting power P_c can be calculated

$$M_c = F_{op} \cdot \frac{d}{2} \quad (9)$$

$$P_c = M_c \cdot \omega \quad (10)$$

where ω is angular speed in rad/s.

The basis of the mechanistic approach is therefore the specific cutting force coefficient k_s in equation 1, which considers various technological parameters as well as the mechanical properties of the wood. In the past, several studies [3] were carried out in which the authors presented the effects of the various factors in the form of tables and diagrams. The user then had to read the individual coefficients from the diagrams based on specific factors and combine them into a general coefficient k_s . This approach is quite time-consuming and unreliable, as the user can easily make mistakes in their calculations.

2. Materials and Methods

As described, the average cutting force F_m for a chip depends directly on the thickness of the chip h_m , the cutting angle relative to the grain φ_m , the sharpness of the knife r_z , the moisture content of the wood u and the density of the wood ρ . Once the cutting force F_m has been determined, the cutting power can be further determined using the Equations (7-10). It is therefore important to first determine the influence of the basic factors on the size of the cutting force. The test procedure is shown in Figure 2. Firstly, the basic parameters on which the model for determining the cutting forces is based are determined. Then the corresponding technological parameters for carrying out the test are determined, whereby the values of the basic parameters correspond to the required parameters. A cutting test is carried out with the technological parameters determined and the cutting power is measured. The average forces F_m per chip are then calculated from the measured power and used to create a model to determine the cutting forces, which in turn is used to create a model to calculate cutting power.

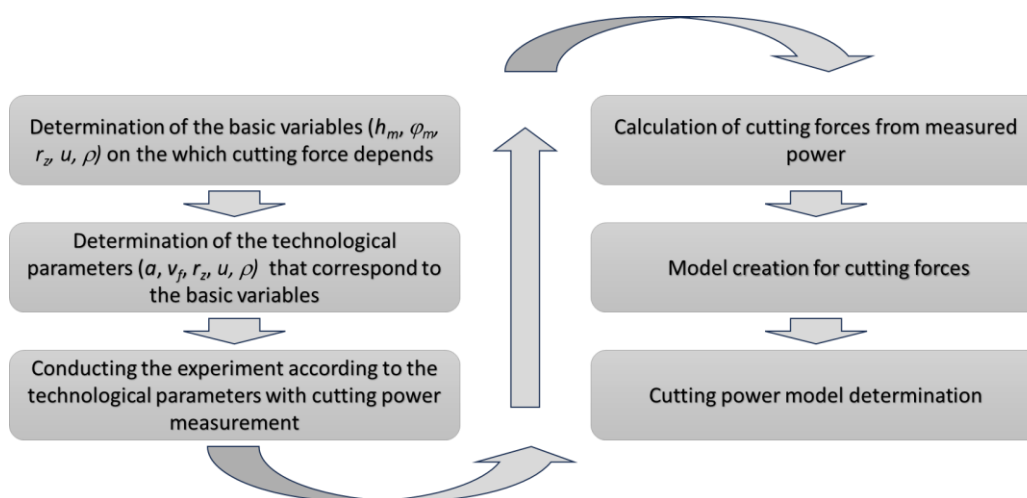


Figure 2. Research process plan.

2.1. Material Preparation

Three tree species with different densities were used for the experiment, namely spruce (*Picea abies*), lime (*Tilia platyphyllos*) and beech (*Fagus sylvatica*). First, samples measuring 750 mm × 100 mm × 30 mm were prepared from boards of different dimensions, which were then equilibrated at standard air conditions of 22°C and 65% relative humidity. After equilibration, the density of the samples was determined and then the density of the absolutely dry wood was calculated. On this basis, the samples were sorted so that their average density was 662.2 kg/m³ for beech, 537.1 kg/m³ for lime and 404.8 kg/m³ for spruce, with standard deviations (SD) of 13.7 kg/m³, 10.7 kg/m³ and 10.5 kg/m³ and coefficient of variations (COV) of 2.07%, 1.99% and 5.06%, respectively. All samples were selected so that the lateral surface that was cut had a radial texture, so that the same amount of earlywood and latewood was cut in each cut. In this way, the influence of the different densities of earlywood and latewood was eliminated. The samples of each tree species were divided into three groups, with one group equilibrated at a relative humidity of 88%, the second group at 67% and the third group at 44%. When the samples had reached the desired equilibrium moisture content (EMC), which averaged 8.1%, 11.9% and 16.2%, the samples were sawn to the final dimensions of 750 mm × 100 mm × 26 mm.

2.2. Cutting Experiment

The cutting experiment was made on an SCM T130 spindle moulder with a feed device Maggi STEFF 2048 connected to a Frenic 5000G11 frequency converter, which allowed the desired feed speeds to be set. A 125 mm diameter cutterhead (Figure 3) with two turnblade knives and a 20° rake angle was used, and the speed was 6000 rpm. As the tool clamp did not have a jointing system that allowed both knives to be set to the same cutting diameter, the experiment was carried out so that

only one knife cut while the cutting edge of the other knife was ground so that the cutting diameter of the second knife was 1 mm smaller than the diameter of the knife that was cutting. Replaceable tungsten carbide cutting inserts measuring 30 mm × 12 mm × 1.5 mm and with a wedge angle of 60° were used in the experiment. Three cutting edge sharpnesses were used. The different sharpenings were achieved by first milling 30 mm thick oak samples with the knife in such a way that the cutting edge was worn down evenly. During the wear process, the radius of the cutting edge was measured using a LEXT OL5000 3D laser scanning microscope, taking 30 measurements along the cutting edge and calculating the average radius value. In the experiment, the knives therefore had average cutting-edge rounding radii of 5.2 μm, 19.1 μm and 34.9 μm, with standard deviations of 1.1 μm, 3.1 μm and 3.1 μm, respectively. As the rake angles in the industry for milling solid wood in longitudinal direction are on average between 18° and 22°, only a rake angle of 20° was used in the experiment, as no significant differences would be recognizable with a smaller rake angle of 18° or a larger one of 22°.



Figure 3. Cutting tool with tungsten carbide knives.

2.3. Planning the Experiment

The Design of Experiments (DOE) method using Design Expert software, Response Surface Modelling (RSM) and Central Composite Design (CCD) was used to plan the experiment and matrix. The CCD method is particularly useful if you want to build a second-order quadratic modelling system, as it allows you to efficiently determine main effects, interactions and curvatures without having to perform a full three-stage factorial experiment, which can be very extensive with a large number of variables [40].

In the experiment, a full factorial rotatable design with the basic part of the 2^k plan with n_k number of factorial points is used with a standard 2-level factorial design at low “-1” and high “+1” levels to determine main effects and interactions. Additional symmetrically arranged axial points n_α are added along each axis at a distance of $\pm\alpha$ around the centre of the plan to capture the curvature of the response. In our case, the experimental design was face-centred with $\alpha=1$. To perform a dispersion analysis of experimental or model results (calculating the error, testing the significance of model coefficients, checking the adequacy and determining the confidence limits of the model, determining the curvature, etc.), the model requires a certain number n_0 of runs at the central values of the variation factors. The use of the system of n_0 runs at the central point is only justified under the assumption that the errors are the same for each run in the covered multifactor space. Normally, the number of central points is 4 to 6, but in this experiment, due to wood variability, eight repetitions were performed at the central point of the plan ($n_0 = 8$) at the central values of the variation factors. In general form, the number of experiments is obtained from the equation

$$N = 2^k + 2k + n_0 = n_k + n_\alpha + n_0 \quad (11)$$

where N is the total of experiments or combinations, k number of parameters, n_k ($n_k=2^k$) number of factorial points, n_α ($n_\alpha=2k$) number of symmetrically placed points around the center of the plan and n_0 number of repetitions at the center point of the plan.

In the experiment 5 factors were included ($k=5$) so the total number of experiments is

$$N = 32 + 10 + 8 = 50$$

In the experiment, the average angle φ_m between the cutting vector and the tissue varied at different cutting depths a , so the calculation of the appropriate depth was performed according to Equations 4 and 5. However, as the mean thickness of the chip h_m increased with increasing depth of cutting, the feed rate also needed to be adjusted to ensure that the mean thickness of the chip met the required conditions. The corresponding feed rate was therefore calculated using equations 2 and 3.

Five variables with three different values were included in the experiment, whereby the minimum and maximum values were taken from the most common process parameters. Their values are listed in Table 1.

Table 1. Real value parameters and parameters used in DOE cutting model.

	Real values		
	min	mean	max
Mean chip thickness, h_m (mm)	0.1	0.25	0.4
Mean cutting angle, φ_m ($^\circ$)	5	15	25
Tool tip radius, r_z (μm)	5.2	19.1	34.9
Wood moisture content, u (%)	8.1	11.9	16.2
Wood density, ρ (kg/m^3)	404.8	537.1	662.2
	Modeled values		
	-1	0	1
Mean chip thickness, h_m (m)	0.0001	0.0003	0.0004
Mean cutting angle, φ_m (rad)	0.08727	0.2618	0.436332
Tool tip radius, r_z (μm)	5	20	35
Wood moisture content, u (%)	8	12	16
Wood density, ρ (kg/m^3)	405	535	665

As it is important for the CCD model used in the experiment that the differences in the values of the individual variables between the minimum and average values and between the average and maximum values are the same, the values given in the lower part of Table 1 were considered in the model. The values used for model differ slightly from the actual values, but the differences are minimal and the values have been converted to base units so that the resulting model can be manipulated more easily.

The experiment combinations with coded, modelled and corresponding technological factors are shown in Table A1 in the Appendix.

2.4. Power Measurements

With the combinations obtained in this way, an experiment was carried out in which three repetitions were performed for each combination. For each repetition, the cutting power was calculated by first measuring the power at idle and then the power during cutting and using the difference to calculate the cutting power.

The power was calculated by measuring the voltage (U) and current (I) on all three phases of the electric motor driving the table cutter. An electrical voltage transformer was used to convert the electrical voltage from the -400 to +400 V range to the -10 to +10 V range, and an electrical current transformer was used to generate a voltage proportional to the current, also in the -10 to +10 V range. All voltages were acquired using a National Instruments NI-USB 6351 acquisition card with a sampling frequency of 2500 Hz and then converted to the real value of voltage and current. National Instruments LabVIEW software was used for acquisition and calculation. The power for each phase was calculated 10 times per second, using 250 samples of U and I for each calculation, by multiplying the instantaneous values of voltage and current for each phase separately. The total power was the sum of the power from all three phases [1].

The cutting power was determined as an average value over the entire length of the workpiece and used to calculate the cutting forces. First M_c from equation 10 and then F_{op} and F_m from Equations 9 and 7 were determined. The mean force per chip F_m was then normalised to a cutting width of 1 m, so that the values were divided by the segment width of 0.026 m. The normalised values F_{mb} were then entered into the Design Expert software, where a detailed ANOVA analysis was performed to determine the significance of the individual parameters and their interactions, and a suitable mathematical model for F_{mb} was created. The model obtained for F_{mb} was then converted into a model for calculating the cutting power P_c using equations 1 to 10, considering the technological parameters and the density and moisture content of the wood in the manner shown in Figure 2.

3. Results and Discussion

The power measurements, together with the average values and coefficient of variations (COV) for individual combinations, where three repetitions were performed for each combination, are shown in Table 2. Individual COV values for all combinations range from 0.26% to 19.88%, with an average COV value of 7.80%. For combinations with standard order (STD) 43 to 50, which belong to group m_0 for the dispersion analysis, and are made at the center point of the plan, the average power value is 877.5 W, the standard deviation 85.03 W and the COV 9.69%. Although the COV values for cutting power are higher than the COV values for wood density, where they averaged 3.04%, they can still be considered low values, as in general the variability of the mechanical properties of wood at the same density can be quite high [27]. The analysis also confirms the fact that a threefold repetition for each combination is sufficient, as the differences between individual measurements are relatively small. The reason for the low COV values can also be attributed to the fact that the surface that was cut had a strictly radial surface, where the amount of early and late wood was always the same during cutting. When cutting a surface with a tangential texture, the differences in power would be much greater for the same combination, as one cut could be mainly earlywood, another mainly latewood and a third a combination of earlywood and latewood. In this case, it would be necessary to perform a larger number of repetitions for the same combination of parameters to obtain a representative average value, as is the case when cutting a surface with radial texture. The table 2 also shows the average power values, the mean forces per chip F_m calculated with equations 7-10 for a chip with a cutting width of 26 mm and the normalised force values F_{mb} for a cutting width of 1 m, which were further used in the model development and the detailed statistical analysis.

The results of the ANOVA analysis is shown in Table 3. The analysis shows that the quadratic equation fits best, as it has the highest R^2 and is also suggested by Design Expert. However, for further analysis, the reduced quadratic equation is used as the use of the quadratic equation can lead to problems when the model is applied outside the tested range, where the positive trend can become negative due to the nature of the quadratic equation. According to studies by cited authors who have investigated the effects of individual parameters, the force increases for all parameters except moisture, where the force initially increases up to a wood moisture content of around 12% and then begins to decrease at higher moisture contents. To obtain a positive trend for all parameters except moisture content, the quadratic terms for all variables except moisture content were removed from the equation so that the model could show an initial increase in force and then a decrease with increasing wood moisture content.

Table 2. Measured power values and corresponding forces.

	Response1	Response2	Response3	Average value	Coefficient of variation (power)	Mean force per chip	Normalized mean force per chip
	P_1	P_2	P_3	P	COV	F_m	F_{mb}
	(W)	(W)	(W)	(W)	(%)	(N)	(N/m)
1	79	83	75	79	4.13	73	2807

2	120	124	103	116	7.87	107	4111
3	127	113	103	114	8.61	106	4064
4	135	118	144	132	8.15	122	4706
5	213	181	181	192	7.87	177	6824
6	255	278	313	282	8.46	261	10045
7	196	222	243	220	8.72	204	7859
8	309	269	283	287	5.77	266	10238
9	96	113	117	109	8.38	100	3864
10	180	179	136	165	12.43	153	5871
11	126	168	148	147	11.64	136	5242
12	162	175	193	177	7.19	163	6287
13	236	213	218	222	4.44	206	7919
14	293	331	387	337	11.46	312	12010
15	249	287	239	258	8.00	239	9178
16	313	305	290	303	3.15	280	10772
17	578	624	671	624	6.08	116	4453
18	858	749	815	807	5.55	150	5762
19	616	604	677	632	5.05	117	4511
20	972	972	864	936	5.44	174	6687
21	1199	1138	1257	1198	4.06	223	8569
22	1509	2082	2492	2028	19.88	378	14557
23	1323	1390	1487	1400	4.81	260	10017
24	2726	2685	2844	2752	2.45	515	19825
25	849	1012	1002	954	7.82	177	6815
26	1141	1091	1195	1142	3.72	212	8158
27	1145	874	871	963	13.34	179	6875
28	1343	1342	1350	1345	0.26	250	9618
29	1434	1782	1245	1487	14.96	277	10651
30	2008	1633	2055	1899	9.95	354	13627
31	2327	1773	2086	2062	11.00	385	14813
32	2550	3121	2675	2782	8.81	521	20023
33	610	678	479	589	14.02	182	7000
34	756	856	986	866	10.87	268	10310
35	656	772	709	712	6.66	220	8477
36	919	988	886	931	4.56	288	11083
37	651	650	619	640	2.32	198	7614
38	972	894	1232	1033	13.99	320	12305
39	626	633	676	645	3.43	199	7673
40	1020	823	828	890	10.30	276	10596
41	224	238	257	240	5.64	222	8534
42	1603	1668	1648	1640	1.66	306	11759
43	890	877	837	868	2.60	269	10335
44	757	805	1019	860	13.24	266	10248
45	833	885	908	875	3.58	271	10422
46	1040	802	809	884	12.51	274	10526
47	894	923	826	881	4.61	273	10492
48	841	774	1045	887	13.00	274	10557
49	843	930	882	885	4.02	274	10537

50	1035	743	863	880	13.61	272	10473
----	------	-----	-----	-----	-------	-----	-------

Table 3. Fit summary for various models

Source	Sequential p-value	Lack of Fit p-value	Adjusted R ²	Predicted R ²	
Linear	< 0.0001	< 0.0001	0.8076	0.7637	
2FI	0.0057	< 0.0001	0.8711	0.7584	
Quadratic	0.0042	< 0.0001	0.914	0.8085	Suggested
Cubic	0.0032	< 0.0001	0.9702	0.3511	Aliased

The ANOVA results of the reduced quadratic equation are shown in Table 4. The Model F-value of 30.82 implies the model is significant. There is only a 0.01% chance that an F-value this large could occur due to noise.

p-values less than 0.05 indicate model terms are significant. In this case A, B, C, D, E, AC, AE, BC, BE, CE and B² are significant model terms. Values greater than 0.10 indicate the model terms are not significant and are removed from the model due to the simplicity of the model.

Table 4. ANOVA analysis for reduced quadratic model.

Source	Sum of Squares	df	Mean Square	F-value	p-value
Model	5.92×10^8	16	3.70×10^7	30.82	< 0.0001
A – ρ	7.69×10^7	1	7.69×10^7	64.04	< 0.0001
B – u	2.19×10^7	1	2.19×10^7	18.22	0.0002
C – h_m	3.05×10^8	1	3.05×10^8	253.64	< 0.0001
D – r	2.58×10^7	1	2.58×10^7	21.47	< 0.0001
E – φ_m	9.35×10^7	1	9.35×10^7	77.85	< 0.0001
AB	3.52×10^5	1	3.52×10^5	0.2933	0.5918
AC	1.61×10^7	1	1.61×10^7	13.4	0.0009
AD	1.06×10^6	1	1.06×10^6	0.8804	0.3549
AE	7.29×10^6	1	7.29×10^6	6.07	0.0192
BC	4.79×10^6	1	4.79×10^6	3.98	0.0543
BD	3.03×10^5	1	3.03×10^5	0.2521	0.6189
BE	6.92×10^6	1	6.92×10^6	5.76	0.0222
CD	6.53×10^5	1	6.53×10^5	0.5431	0.4663
CE	1.42×10^7	1	1.42×10^7	11.81	0.0016
DE	1.02×10^6	1	1.02×10^6	0.8485	0.3637
B ²	1.69×10^7	1	1.69×10^7	14.06	0.0007

The resulting model for calculating the F_{mb} for coded and actual factors is shown in Table 5. In the case of coded factors, the coded values of the variables, i.e. -1, 0 and 1, must be used for the calculation. The advantage of coded factors is that they show the relative importance of individual variables or combinations of variables. For example, it can be deduced from the coded factors that the thickness of the chip h_m , whose coded factor has the highest value, has the greatest influence on the cutting forces, followed by the φ_m , ρ , r_z , and u . The model is also influenced by the interaction of various variables with approximately equal effects.

Table 5. Coefficient in terms of coded and actual factors.

coded factors	actual factors
---------------	----------------

F_{mb}	=	F_{mb}	=
+9961.31		-4986.22	
+1504.25	A - ρ	-3.028	ρ
+802.31	B - u	+1733.99	u
+2993.67	C - h_m	-1.389×10^7	h_m
+870.91	D - r_z	+58.060	r_z
+1658.50	E - φ_m	-16104.52	φ_m
+709.27	AC	+36372.87	$\rho * h_m$
+477.19	AE	+21.03	$\rho * \varphi_m$
+386.71	BC	$+6.44 \times 10^5$	$u * h_m$
+465.17	BE	+666.32	$u * \varphi_m$
+665.93	CE	$+2.54 \times 10^7$	$h_m * \varphi_m$
-1245.99	B ²	-77.87	u^2

Table 6 shows the model fit statistics, where R^2 , Adjusted R^2 , and Predicted R^2 are 0.9319, 0.9122, and 0.866, respectively. The Predicted R^2 of 0.866 is in reasonable agreement with the Adjusted R^2 of 0.9122 where the difference is less than 0.2. Also Adeq Precision which should be greater than 4 and measures the signal to noise ratio is 30.22, which indicates an adequate signal and model can be used to navigate the design space, while coefficient of variation is 11.68 %, which is also acceptable.

Table 6. Fit statistics.

R^2	Adjusted R^2	Predicted R^2	Adeq Precision	Std. Dev.	Mean	C.V. %
0.9319	0.9122	0.866	30.2287	1064.11	9114.03	11.68

The relationship between the measured and calculated F_{mb} is shown in Figure 4a. The linear trend between them is obvious and confirms the suitability of the model for calculating the cutting forces, which is also confirmed by the normal curve of the residuals (Figure 4b), which also runs around the straight line. Figure 4c shows that the values are within the residual limits and have a random distribution, while Figure 4d shows that the residuals do not depend on the number of runs.

The effects of the various factors and their interactions are shown in Figure 5. The trend of a particular factor depends on the value of another factor with which the first factor interacts. F_{mb} increases faster with increasing h_m at higher ρ than at lower ρ (Figure 5a). The same is true for the increase in F_{mb} with a change in φ_m , with F_{mb} also increasing faster at a higher ρ than at a lower ρ (Figure 5b). The effect of moisture content on the F_{mb} can be seen in Figure 5c, where F_{mb} increases faster with h_m in moist wood than in dry wood, and the F_{mb} also increases faster with φ_m in moist wood than in dry wood (Figure 5d). Looking at moisture content, F_{mb} initially increases with u up to a certain value and then starts to decrease as u increases further (Figure 5d), which is also consistent with the trend of other mechanical properties [41] that initially increase up to a certain moisture content and then decrease as the moisture content of the wood increases. There is also an interaction between φ_m and h_m (Figure 5e), with F_{mb} increasing faster with h_m in a more transverse cut (bigger φ_m) than in a longitudinal cut (smaller φ_m). The perturbation plot in coded values, which shows how the response changes as each factor moves away from the chosen reference point while all other factors are held constant at the reference value in the centre of the design space, is shown in Figure 5f. The figure clearly shows that factor C has the largest slope and therefore the largest influence on the increase in F_{mb} , followed by factors E, A, D and B, as already shown in Table 5.

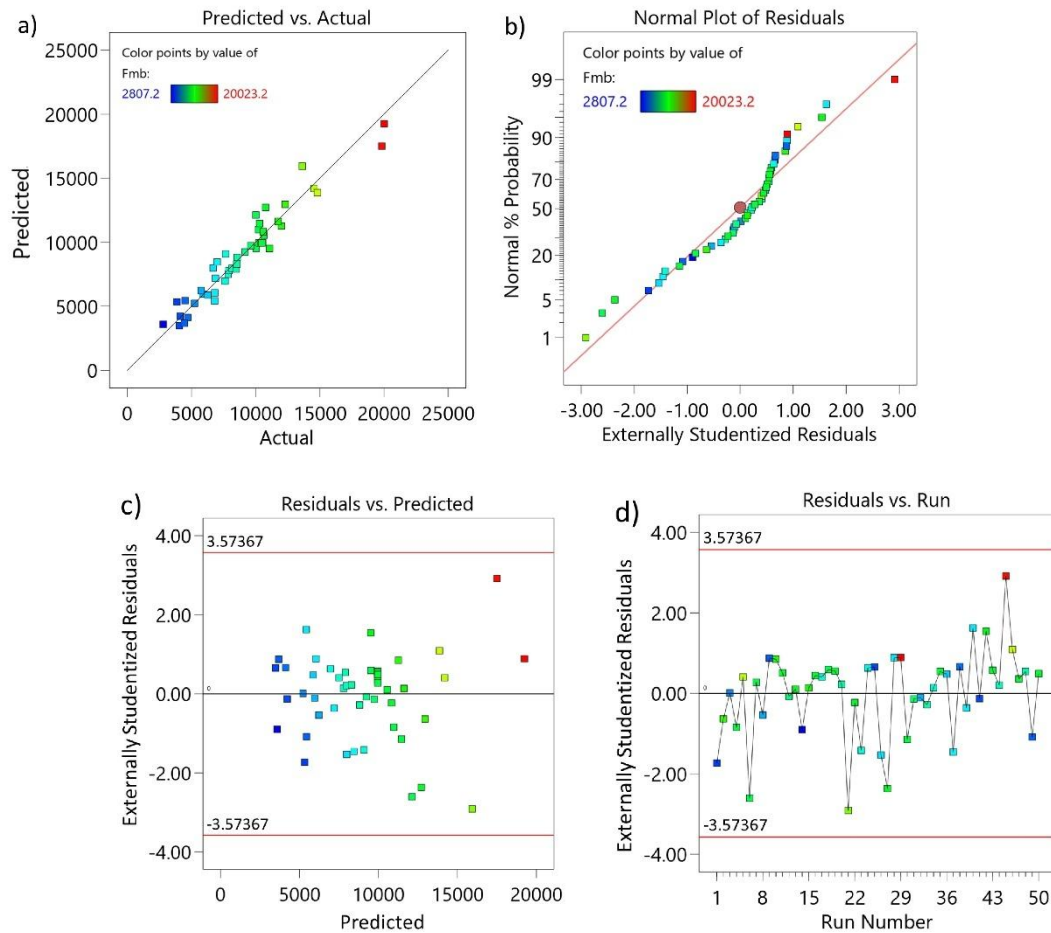
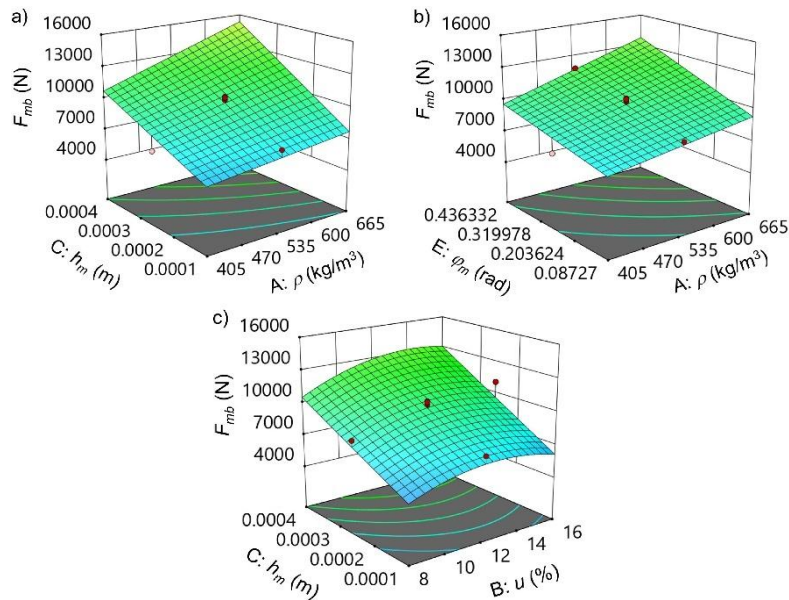


Figure 4. Plots of model adequacy; a) Actual and predicted cutting forces F_{mb} , and b) normal plot of residuals, c) plots of residuals vs. predicted values, and d) plots of residuals vs. run.



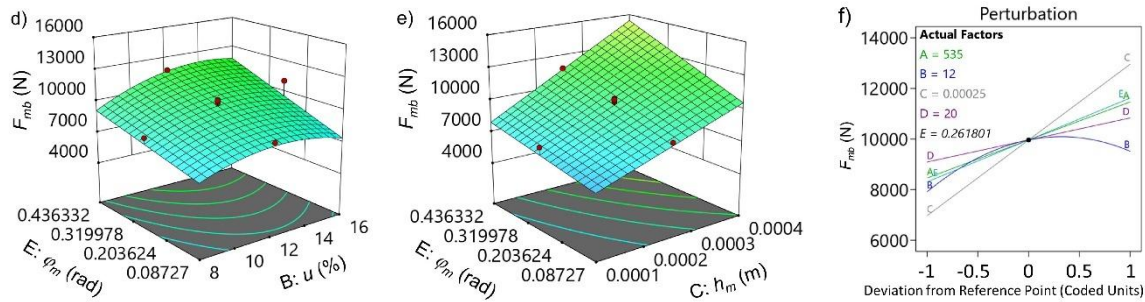


Figure 5. Interactions of the experimental factors on cutting force F_{mb} : a) wood density ρ and mean chip thickness h_m , b) wood density ρ and mean cutting angle φ_m , c) wood moisture content u and mean chip thickness h_m , d) wood moisture content u and mean cutting angle φ_m , e) mean chip thickness h_m and mean cutting angle φ_m and f) perturbation plot of factors.

To obtain the model for calculating the cutting power with actual technological parameters, the equation on the right-hand side of Table 5 must be considered. Then the equation must be multiplied by the cutting width (b) and then equations 2 and 3 for h_m and equations 4 and 6 for φ_m must be used. In addition, the resulting equation must be multiplied by the average number of knives (z_{ef}) cutting per unit time (Eq. 7), the tool diameter (d) and the angular velocity (ω) using equations 9 and 10. After rearranging the equation so that practical units can be used, the final model for calculating the power of peripheral cutting of solid wood in longitudinal direction with a knife having a rake angle of 20° (or approximately 20°) can be written as follows

$$P_c = b \left[a \left(nz(-0.000268 + 0.0000111u + 3.5 \times 10^{-7}\rho) + v_f(-0.231 + 0.4239\sqrt{\frac{a}{d}} + 0.01074u + 0.000606\rho) \right) + nz\sqrt{ad}(-0.0000831 + 9.676 \times 10^{-7}r_z + 0.0000288u - 0.000001297u^2 - 5.047 \times 10^{-8}\rho) \right] \quad (13)$$

where b is the cutting width in mm, a the cutting depth in mm, d the tool diameter in mm, n the tool rotational speed in rpm, z the number of tool knives, v_f the feed speed in m/min, r_z the blade sharpness radius in μm , u the wood moisture content in % and ρ the wood density in kg/m^3 .

The verification of the model is shown in Table 7, which shows the power calculations based on the model (Eq. 13) and the measured values. The difference between the calculated and measured values is on average 8.8 %, which is a relatively small deviation, especially considering the relatively high variability of density within tree species and, at the same density, the variability of mechanical properties [27] that actually affect the force and thus the cutting power [14].

Table 7. Actual and predicted values of cutting power and their differences.

STD	Actual values -	Predicted values -	Difference	STD	Actual values -	Predicted values -	Difference
	P	P_c			P	P_c	
	(W)	(W)	(%)		(W)	(W)	(%)
1	79.0	101.8	28.9	26	1142.3	1131.2	1.0
2	115.7	119.9	3.6	27	963.3	1020.2	5.9
3	114.3	99.0	13.4	28	1345.0	1381.1	2.7
4	132.3	117.1	11.5	29	1487.0	1497.6	0.7
5	191.7	171.7	10.4	30	1898.7	2260.8	19.1
6	282.0	270.2	4.2	31	2062.0	1966.8	4.6
7	220.3	212.8	3.4	32	2782.0	2730.0	1.9
8	287.0	311.3	8.5	33	589.0	719.4	22.1
9	108.7	151.3	39.2	34	866.0	975.3	12.6

10	165.0	169.3	2.6	35	712.3	673.1	5.5
11	147.3	148.4	0.8	36	931.0	809.6	13.0
12	176.7	166.5	5.8	37	640.0	592.7	7.4
13	222.3	221.1	0.5	38	1032.7	1102.0	6.7
14	337.0	319.7	5.1	39	645.0	773.3	19.9
15	258.3	262.2	1.5	40	890.3	921.5	3.5
16	302.7	360.7	19.2	41	239.7	235.5	1.7
17	624.3	523.4	16.2	42	1639.7	1647.9	0.5
18	807.3	884.2	9.5	43	868.0	847.4	2.4
19	632.3	773.2	22.3	44	860.3	847.4	1.5
20	936.0	1134.0	21.2	45	875.3	847.4	3.2
21	1198.0	1250.5	4.4	46	883.7	847.4	4.1
22	2027.7	2013.7	0.7	47	881.0	847.4	3.8
23	1400.0	1719.7	22.8	48	886.7	847.4	4.4
24	2751.7	2482.9	9.8	49	885.0	847.4	4.3
25	954.3	770.4	19.3	50	880.3	847.4	3.7

4. Conclusions

In the study, a model was developed to calculate the power required for circular cutting of solid wood in the longitudinal direction. The experiment was designed and conducted with five input parameters, which were varied in three levels. The model is essentially based on the thickness of the chip, the cutting angle between the speed vector of the knives and the orientation of the wood tissue, the sharpness of the knives and the density and moisture content of the wood. Using geometric and kinematic relationships, a model is then derived that contains the following actual technological parameters: cutting width and depth, tool diameter and speed, number and sharpness of the knives as well as feed rate, density and moisture content of the workpiece.

The developed model can be used to calculate the cutting power of various tree species with densities ranging from 400 kg/m³ to 700 kg/m³, moisture contents from 8% to 16%, and a wide range of cutting edge sharpness, from a sharp cutting edge with a tip radius of 5 µm to a blunt cutting edge with a tip radius of 35 µm.

A detailed statistical analysis of the test results and a comparative analysis of the modelled and experimental values of the cutting forces from the test confirmed that the derived model is highly significant. The developed model is simple and robust and allows the calculation of the cutting power with an average accuracy of 8.8%, which is a relatively high accuracy, especially considering the high variability of mechanical properties for a given tree species or wood density.

The model represents a significant contribution as, to the authors' knowledge, there is currently no such comprehensive, robust and simple model available in the literature that considers all important technological parameters as well as basic wood properties such as wood density and moisture content.

However, the model developed can only be used for peripheral cutting of solid wood in the longitudinal direction and is not suitable for composite materials or for cutting solid wood in the perpendicular direction. In the first case, the mechanical properties can be very different from those of solid wood, and in the second case, the properties of solid wood in the transverse direction are just as different as in the longitudinal direction.

The model developed is based on a rake angle of 20°, which on average is the most commonly used angle for machining solid wood in the longitudinal direction and is therefore not suitable for knives with significantly smaller or larger rake angles.

Author Contributions: Conceptualization, M.M., D.H., N.H., and A.H; methodology, M.M., D.H., R.H., N.H., and A.H; validation, M.M., D.H., N.H., and A.H; formal analysis, M.M., D.H., N.H., and A.H; investigation, M.M., D.H., R.H., N.H. and A.H; resources, M.M., N.H., and A.H; writing—original draft preparation, M.M. and

A.H.; writing—review and editing, M.M., D.H., and N.H.; visualization, M.M. and N.H.; supervision, M.M., D.H. and A.H.; project administration, M.M., D.H. and A.H.; funding acquisition, M.M., R.H. and A.H. All authors have read and agreed to the published version of the manuscript.

Funding: The work was supported by the Slovenian Research Agency under Grant P2-0182 Programs and Ministry of Science and Education of Federation B&H under Grant Nr.05-35-4925-1/24.

Data Availability Statement: No new data were created.

Acknowledgments: The authors acknowledge the support the Ministry of Science and Education of the Federation of Bosnia and Herzegovina and the United Nations Development Programme (UNDP) through the national project “Optimization of Solid Wood Processing Parameters” (Grant No. 05-35-4925-1/24) and Faculty of Technical Engineering, University of Bihać.

Conflicts of Interest: The authors declare no conflicts of interest.

Appendix A

Table A1. Coded and modelled factors together with corresponding technological factors.

STD	Coded factors					Modelled factors					Corresponding technological factors				
	Density	Humidity	Chip thickness	Cutting edge radius	Mean cutting angle	Density	Humidity	Chip thickness	Cutting edge radius	Mean cutting angle	Density	Humidity	Feed rate	Cutting edge radius	Cutting depth
	ρ	u	h_m	r_z	φ_m	ρ (kg/m ³)	u (%)	h_m (m)	r_z (μ m)	φ_m (rad)	ρ (kg/m ³)	u (%)	v_f (m/min)	r_z (μ m)	a (mm)
1	-1	-1	-1	-1	-1	405	8	0.0001	5	0.0873	405	8	13.8	5	0.95
2	1	-1	-1	-1	-1	665	8	0.0001	5	0.0873	665	8	13.8	5	0.95
3	-1	1	-1	-1	-1	405	16	0.0001	5	0.0873	405	16	13.8	5	0.95
4	1	1	-1	-1	-1	665	16	0.0001	5	0.0873	665	16	13.8	5	0.95
5	-1	-1	1	-1	-1	405	8	0.0004	5	0.0873	405	8	55.0	5	0.95
6	1	-1	1	-1	-1	665	8	0.0004	5	0.0873	665	8	55.0	5	0.95
7	-1	1	1	-1	-1	405	16	0.0004	5	0.0873	405	16	55.0	5	0.95
8	1	1	1	-1	-1	665	16	0.0004	5	0.0873	665	16	55.0	5	0.95
9	-1	-1	-1	1	-1	405	8	0.0001	35	0.0873	405	8	13.8	35	0.95
10	1	-1	-1	1	-1	665	8	0.0001	35	0.0873	665	8	13.8	35	0.95
11	-1	1	-1	1	-1	405	16	0.0001	35	0.0873	405	16	13.8	35	0.95
12	1	1	-1	1	-1	665	16	0.0001	35	0.0873	665	16	13.8	35	0.95
13	-1	-1	1	1	-1	405	8	0.0004	35	0.0873	405	8	55.0	35	0.95
14	1	-1	1	1	-1	665	8	0.0004	35	0.0873	665	8	55.0	35	0.95
15	-1	1	1	1	-1	405	16	0.0004	35	0.0873	405	16	55.0	35	0.95
16	1	1	1	1	-1	665	16	0.0004	35	0.0873	665	16	55.0	35	0.95
17	-1	-1	-1	-1	1	405	8	0.0001	5	0.4364	405	8	2.8	5	22.33
18	1	-1	-1	-1	1	665	8	0.0001	5	0.4364	665	8	2.8	5	22.33
19	-1	1	-1	-1	1	405	16	0.0001	5	0.4364	405	16	2.8	5	22.33
20	1	1	-1	-1	1	665	16	0.0001	5	0.4364	665	16	2.8	5	22.33
21	-1	-1	1	-1	1	405	8	0.0004	5	0.4364	405	8	11.2	5	22.33
22	1	-1	1	-1	1	665	8	0.0004	5	0.4364	665	8	11.2	5	22.33
23	-1	1	1	-1	1	405	16	0.0004	5	0.4364	405	16	11.2	5	22.33

24	1	1	1	-1	1	665	16	0.0004	5	0.4364	665	16	11.2	5	22.33
25	-1	-1	-1	1	1	405	8	0.0001	35	0.4364	405	8	2.8	35	22.33
26	1	-1	-1	1	1	665	8	0.0001	35	0.4364	665	8	2.8	35	22.33
27	-1	1	-1	1	1	405	16	0.0001	35	0.4364	405	16	2.8	35	22.33
28	1	1	-1	1	1	665	16	0.0001	35	0.4364	665	16	2.8	35	22.33
29	-1	-1	1	1	1	405	8	0.0004	35	0.4364	405	8	11.2	35	22.33
30	1	-1	1	1	1	665	8	0.0004	35	0.4364	665	8	11.2	35	22.33
31	-1	1	1	1	1	405	16	0.0004	35	0.4364	405	16	11.2	35	22.33
32	1	1	1	1	1	665	16	0.0004	35	0.4364	665	16	11.2	35	22.33
33	-1	0	0	0	0	405	12	0.00025	20	0.2617	405	12	11.5	20	8.37
34	1	0	0	0	0	665	12	0.00025	20	0.2617	665	12	11.5	20	8.37
35	0	-1	0	0	0	535	8	0.00025	20	0.2617	535	8	11.5	20	8.37
36	0	1	0	0	0	535	16	0.00025	20	0.2617	535	16	11.5	20	8.37
37	0	0	-1	0	0	535	12	0.0001	20	0.2617	535	12	4.6	20	8.37
38	0	0	1	0	0	535	12	0.0004	20	0.2617	535	12	18.4	20	8.37
39	0	0	0	-1	0	535	12	0.00025	5	0.2617	535	12	11.5	5	8.37
40	0	0	0	1	0	535	12	0.00025	35	0.2617	535	12	11.5	35	8.37
41	0	0	0	0	-1	535	12	0.00025	20	0.0873	535	12	34.4	20	0.95
42	0	0	0	0	1	535	12	0.00025	20	0.4364	535	12	7.0	20	22.33
43	0	0	0	0	0	535	12	0.00025	20	0.2617	535	12	11.5	20	8.37
44	0	0	0	0	0	535	12	0.00025	20	0.2617	535	12	11.5	20	8.37
45	0	0	0	0	0	535	12	0.00025	20	0.2617	535	12	11.5	20	8.37
46	0	0	0	0	0	535	12	0.00025	20	0.2617	535	12	11.5	20	8.37
47	0	0	0	0	0	535	12	0.00025	20	0.2617	535	12	11.5	20	8.37
48	0	0	0	0	0	535	12	0.00025	20	0.2617	535	12	11.5	20	8.37
49	0	0	0	0	0	535	12	0.00025	20	0.2617	535	12	11.5	20	8.37
50	0	0	0	0	0	535	12	0.00025	20	0.2617	535	12	11.5	20	8.37

References

1. Merhar, M.; Bjelić, A.; Hodžić, A. Modelling of Peripheral Wood Milling Power Using Design of Experiment Approach. *Drv. Ind.* **2024**, *75*, 395-404, doi:10.5552/drvind.2024.0173.
2. Ettelt, B. Sägen, Fräsen, Hobeln, Bohren : die Spannung von Holz und ihre Werkzeuge, 3rd ed.; DRW-Verlag: Stuttgart, 2004.
3. Kivimaa, E. Die Schnittkraft in der Holzbearbeitung. *Holz als Roh- und Werkstoff: European Journal of Wood and Wood Industries* **1952**, *10*, 94-108, doi:10.1007/BF02608840.
4. Wellenreiter, P.; Hernández, R.E.; Cáceres, C.B.; Blais, C. Cutting forces and noise in helical planing black spruce wood as affected by the helix angle and feed per knife. *Wood Material Science & Engineering* **2023**, *18*, 549-558, doi:10.1080/17480272.2022.2056079.
5. Li, R.R.; He, C.J.; Xu, W.; Wang, X.D. Modeling and optimizing the specific cutting energy of medium density fiberboard during the helical up-milling process. *Wood Material Science & Engineering* **2023**, *18*, 464-471, doi:10.1080/17480272.2022.2049867.
6. Yaghoubi, S.; Rabiei, F.; Seidi, M. A comprehensive assessment on surface quality of machined wooden products via Box-Behnken design method. *Wood Material Science & Engineering* **2024**, *19*, 896-905, doi:10.1080/17480272.2023.2290212.
7. Xu, W.; Wu, Z.; Lu, W.; Yu, Y.; Wang, J.; Zhu, Z.; Wang, X. Investigation on Cutting Power of Wood-Plastic Composite Using Response Surface Methodology. *Forests* **2022**, *13*, doi:10.3390/f13091397.
8. Zhu, Z.L.; Buck, D.; Song, M.Q.; Tang, Q.; Guan, J.; Zhou, X.L.; Guo, X.L. Enhancing face-milling efficiency of wood-plastic composites through the application of genetic algorithm-back propagation neural network.

- Wood Material Science & Engineering* **2024**, 10.1080/17480272.2024.2388844, doi:10.1080/17480272.2024.2388844.
9. Blackman, B.R.K.; Houlst, T.R.; Patel, Y.; Williams, J.G. Tool sharpness as a factor in machining tests to determine toughness. *Engineering Fracture Mechanics* **2013**, *101*, 47-58, doi:10.1016/j.engfracmech.2012.09.020.
 10. Merhar, M.; Bucar, B. Friction in linear orthogonal cutting of beech wood (*fagus sylvatica*) considering ploughing effect forces due to cutting tool tip bluntness. *Wood Res.* **2013**, *58*, 319-328.
 11. Li, W.G.; Zhu, Z.; Zhang, B. Simulation analysis and experimental research of friction performance between wood and cemented carbide surface with different micro-textures. *Wood Material Science & Engineering* **2024**, 10.1080/17480272.2024.2425799, doi:10.1080/17480272.2024.2425799.
 12. Merhar, M.; Bucar, B. Cutting force variability as a consequence of exchangeable cleavage fracture and compressive breakdown of wood tissue. *Wood Sci. Technol.* **2012**, *46*, 965-977, doi:10.1007/s00226-011-0457-4.
 13. Matsuda, Y.; Fujiwara, Y.; Fujii, Y. Observation of machined surface and subsurface structure of hinoki (*Chamaecyparis obtusa*) produced in slow-speed orthogonal cutting using X-ray computed tomography. *J. Wood Sci.* **2015**, *61*, 128-135, doi:10.1007/s10086-014-1457-4.
 14. Koch, P. *Utilization of the Southern Pines*, 1st ed.; U.S. Southern Forest Experiment Station: New Orleans, 1972.
 15. Elloumi, I.; Hernández, R.E.; Cáceres, C.B.; Blais, C. Effects of log temperature, moisture content, and cutting width on energy requirements for processing logs by a chipper-canter. *Wood Material Science & Engineering* **2023**, *18*, 394-401, doi:10.1080/17480272.2022.2037705.
 16. Minagawa, M.; Matsuda, Y.; Fujiwara, Y.; Fujii, Y. Relationship between crack propagation and the stress intensity factor in cutting parallel to the grain of hinoki (*Chamaecyparis obtusa*). *J. Wood Sci.* **2018**, *64*, 758-766, doi:10.1007/s10086-018-1760-6.
 17. Aboussafy, C.; Guilbault, R. Chip formation in machining of anisotropic plastic materials—a finite element modeling strategy applied to wood. *International Journal of Advanced Manufacturing Technology* **2021**, *114*, 1471-1486, doi:10.1007/s00170-021-06950-6.
 18. Su, Q.; Yu, Z.; Zhang, J.; Liu, W.; Ma, X.; Liu, Z. Mechanisms and influencing factors of branch fracture in Caragana korshinskii: a numerical simulation using XFEM. *Wood Sci. Technol.* **2025**, *59*, doi:10.1007/s00226-025-01672-4.
 19. Matsuda, Y.; Fujiwara, Y.; Murata, K.; Fujii, Y. Residual strain analysis with digital image correlation method for subsurface damage evaluation of hinoki (*Chamaecyparis obtusa*) finished by slow-speed orthogonal cutting. *J. Wood Sci.* **2017**, *63*, 615-624, doi:10.1007/s10086-017-1659-7.
 20. Chuchala, D.; Huang, Y.; Orłowski, K.A.; Buck, D.; Stenka, D.; Fredriksson, M.; Svensson, M. Fracture toughness and shear yield stress determination from quasi-linear cutting tests of Scots pine (*Pinus sylvestris* L.) with a normalisation process by local density aided by X-ray computed tomography. *Eur. J. Wood Wood Prod.* **2025**, *83*, doi:10.1007/s00107-025-02305-0.
 21. Hlášková, L.; Procházka, J.; Novák, V.; Čermák, P.; Kopecký, Z. Interaction between thermal modification temperature of spruce wood and the cutting and fracture parameters. *Materials* **2021**, *14*, doi:10.3390/ma14206218.
 22. Yang, C.; Liu, T.; Ma, Y.; Qu, W.; Ding, Y.; Zhang, T.; Song, W. Study of the Movement of Chips during Pine Wood Milling. *Forests* **2023**, *14*, doi:10.3390/f14040849.
 23. Kubík, P.; Šebek, F.; Krejčí, P.; Brabec, M.; Tippner, J.; Dvořáček, O.; Lechowicz, D.; Frybort, S. Linear woodcutting of European beech: experiments and computations. *Wood Sci. Technol.* **2023**, *57*, 51-74, doi:10.1007/s00226-022-01442-6.
 24. Radmanovic, K.; Dukic, I.; Merhar, M.; Safran, B.; Jug, M.; Lucic, R.B. Longitudinal and Tangential Coefficients of Chip Compression in Orthogonal Wood Cutting. *Bioresources* **2018**, *13*, 7998-8011, doi:10.15376/biores.13.4.7998-8011.
 25. Liao, Z.; Axinte, D.A. On chip formation mechanism in orthogonal cutting of bone. *International Journal of Machine Tools and Manufacture* **2016**, *102*, 41-55, doi:10.1016/j.ijmachtools.2015.12.004.

26. Wang, H.; Satake, U.; Enomoto, T. Serrated chip formation mechanism in orthogonal cutting of cortical bone at small depths of cut. *Journal of Materials Processing Technology* **2023**, *319*, doi:10.1016/j.jmatprotec.2023.118097.
27. Kollmann, F.F.P.; Côte, W.A. *Principles of Wood Science and Technology. Solid Wood.*; Springer-Verlag: Berlin, Germany, 1975; pp. 592
28. Jiang, S.; Buck, D.; Tang, Q.; Guan, J.; Wu, Z.; Guo, X.; Zhu, Z.; Wang, X. Cutting Force and Surface Roughness during Straight-Tooth Milling of Walnut Wood. *Forests* **2022**, *13*, doi:10.3390/f13122126.
29. Pinkowski, G.; Piernik, M.; Wołpiuk, M.; Krauss, A. Effect of Chip Thickness and Tool Wear on Surface Roughness and Cutting Power during Up-Milling Wood of Different Density. *BioResources* **2024**, *19*, 9234-9248, doi:10.15376/BIORES.19.4.9234-9248.
30. Homkhiew, C.; Cheewawuttipong, W.; Srivabut, C.; Boonchouytan, W.; Rawangwong, S. Machinability of wood-plastic composites from the CNC milling process using the Box-Behnken design and response surface methodology for building applications. *Journal of Thermoplastic Composite Materials* **2025**, *38*, 161-187, doi:10.1177/08927057241248036.
31. Dvoracek, O.; Lechowicz, D.; Haas, F.; Frybort, S. Cutting force analysis of oak for the development of a cutting force model. *Wood Mat. Sci. Eng.* **2022**, *17*, 771-782, doi:10.1080/17480272.2021.1955296.
32. Jin, D.; Wei, K. Machinability of Scots Pine during Peripheral Milling with Helical Cutters. *Bioresources* **2021**, *16*, 8172-8183, doi:10.15376/biores.16.4.8172-8183.
33. Li, R.; Yang, F.; Wang, X. Modeling and Predicting the Machined Surface Roughness and Milling Power in Scot's Pine Helical Milling Process. *Machines* **2022**, *10*, doi:10.3390/machines10050331.
34. Porankiewicz, B.; Axelsson, B.; Grönlund, A.; Marklund, B. Main and normal cutting forces by machining wood of *Pinus sylvestris*. *BioResources* **2011**, *6*, 3687-3713.
35. Derbas, M.; Young, T.M.; Frömel-Frybort, S.; Möhring, H.C.; Riegler, M. Predicting wood moisture classes by sound frequency spectra and Explainable Machine Learning during milling. *Wood Mat. Sci. Eng.* **2024**, *10.1080/17480272.2024.2420732*, doi:10.1080/17480272.2024.2420732.
36. Chuchala, D.; Orłowski, K.A.; Sinn, G.; Konopka, A. Comparison of the fracture toughness of pine wood determined on the basis of orthogonal linear cutting and frame sawing. *Acta Facultatis Xylologiae Zvolen* **2021**, *63*, 75-83, doi:10.17423/afx.2021.63.1.07.
37. Zhao, L.; Yuan, W.; Xu, L.; Jin, S.; Cui, W.; Xue, J.; Zhou, H. Linear Cutting Performance Tests and Parameter Optimization of Poplar Branches Based on RSM and NSGA-II. *Forests* **2024**, *15*, doi:10.3390/f15010146.
38. Yang, C.; Ma, Y.; Liu, T.; Ding, Y.; Qu, W. Experimental Study of Surface Roughness of Pine Wood by High-Speed Milling. *Forests* **2023**, *14*, doi:10.3390/f14061275.
39. Goli, G.; Fioravanti, M.; Marchal, R.; Uzielli, L.; Busoni, S. Up-milling and down-milling wood with different grain orientations-the cutting forces behaviour. *Eur. J. Wood Wood Prod.* **2010**, *68*, 385-395, doi:10.1007/s00107-009-0374-5.
40. Montgomery, D.C. *Design and Analysis of Experiments*; John Wiley & Sons, Inc.: Arizona State University, 2013.
41. Brémaud, I.; Gril, J. Moisture content dependence of anisotropic vibrational properties of wood at quasi equilibrium: Analytical review and multi-trajectories experiments. *Holzforschung* **2021**, *75*, 313-327, doi:10.1515/hf-2020-0028.

Disclaimer/Publisher's Note: The statements, opinions and data contained in all publications are solely those of the individual author(s) and contributor(s) and not of MDPI and/or the editor(s). MDPI and/or the editor(s) disclaim responsibility for any injury to people or property resulting from any ideas, methods, instructions or products referred to in the content.